Lactoperoxidase-Catalyzed Oxidation of Thiocyanate by Hydrogen Peroxide: A Reinvestigation of Hypothiocyanite by Nuclear Magnetic Resonance and Optical Spectroscopy†

Péter Nagy, Susan S. Alguindigue, and Michael T. Ashby*

Department of Chemistry and Biochemistry, University of Oklahoma, Norman, Oklahoma 73019

Received May 22, 2006; Revised Manuscript Received August 17, 2006

ABSTRACT: In an effort to reconcile conflicting reports regarding the spectra of the human defense factor hypothiocyanite ($OSCN^-$), we have synthesized $OSCN^-$ by three methods and characterized the product spectroscopically. Method I is lactoperoxidase-catalyzed oxidation of SCN^- by H_2O_2 at pH 7. Method II is hydrolysis of $(SCN)_2$ at pH 13. Method III is oxidation of SCN^- by OX^- (X = Cl and Br) at pH 13. All three methods produced essentially the same initial UV, ^{13}C NMR, and ^{15}N NMR spectra. The UV spectrum reveals a λ_{max} of 376 nm, which is a previously unreported distinguishing feature. The ^{13}C NMR spectrum (δ = 127.8 ppm at pH 13 vs dioxane at 66.6 ppm) is comparable to those that have been previously reported for $OSCN^-$ as prepared by methods I and II (although in some cases different assignments have been made). However, the ^{15}N NMR spectrum we measure (δ = −80.6 ppm at pH 13 vs NO_3^- at 0 ppm) contrasts with previous reports. We conclude that all three methods produce the same species, and the spectra are now self-consistent with the formulation $OSCN^-$.

Secretory proteins play essential roles in human host defense. In addition to the proteins that are associated with immune response, innate antimicrobial proteins augment the defensive stratagems. Perhaps the most widely studied secretory protein is lactoperoxidase (LPO,[1] EC 1.11.1.7). LPO is a heme oxidoreductase that catalyzes the oxidation of a wide variety of substrates by hydrogen peroxide (*1*). The catalytic mechanism can generally be described as a two-electron oxidation of LPO to produce Compound I (LPO-I), followed by transfer of an O atom to the substrate: LPO + H_2O_2 → LPO-I followed by LPO-I + X → LPO + OX (*2*). Thus, substrate selectivity is determined by the rate of the reaction of LPO-I with potential substrates, which in turn is a function of the rate constants for the second step of the mechanism and the concentrations of the substrates in various physiologic fluids (*2*). Although the halides bromide (Br^-) and iodide (I^-) react with LPO-I with significant rates, the pseudo-halide thiocyanate (SCN^-) is generally more abundant in physiologic fluids, and the latter is believed to be the exclusive substrate of LPO in vivo (*2*). The LPO system produces short-lived intermediary oxidation products of SCN^- that provide antibacterial activity. The major species is thought to be hypothiocyanite, which is generally formulated as $OSCN^-$, although alternative molecular structures have been proposed (vide infra). In addition to the enzymic method of producing hypothiocyanite, the same species is apparently obtained by the hydrolysis of thiocyanogen, $(SCN)_2$ (*3*). Furthermore, we have recently prepared hypothiocyanite through the uncatalyzed oxidation of SCN^- by hypohalous acids, HOX (X = Cl and Br) (*4*, *5*). The action of hypothiocyanite against bacteria is believed to be caused by sulfhydryl oxidation (*6*−*8*) vis-à-vis sulfenyl thiocyanates (RSSCN), which subsequently hydrolyze to sulfenic acids that produce a cascade of reactive sulfur species (*9*). While it is recognized that reagents that target sulfhydryl groups render a majority of proteins inactive (*10*), a fact that would explain the biocidal properties of hypothiocyanite, it is unclear what chemical properties of hypothiocyanite give rise to the observed selectivity between prokaryotes and eukaryotes (*11*).

Hypothiocyanite is a highly reactive chemical species that has never been isolated in a pure form; however, it has been the subject of extensive theoretical (*12*−*14*) and spectroscopic investigation (*15*−*21*). Early molecular orbital calculations by Pyykko and Runeberg predicted that the relative thermodynamic stabilities of the isomers of hypothiocyanite (in the gas phase) decrease in the following order: $OCNS^-$ > $ONCS^-$ > $OSCN^-$ (*12*). However, it was subsequently concluded by Sundholm that the computed relative thermodynamic stabilities (in the gas phase) of the isomers decrease in the following order: $OCNS^-$ > $OSCN^-$ > $ONCS^-$ (*13*). A recent study by Dua et al. included additional isomers: $OCNS^-$ > $SOCN^-$ > $OSCN^-$ > $ONCS^-$ > $OSNC^-$ (*14*). The ultraviolet (UV) spectrum of hypothiocyanite in aqueous solution has been measured under various conditions (*15*, *20*), but the electronic spectrum does not differentiate between the possible isomers. In an effort to distinguish

† This work was supported by the National Science Foundation (CHE-0503984), the American Heart Association (0555677Z), the National Institutes of Health (5 P20 RR018741-02), and the Petroleum Research Fund (42850-AC4).

* To whom correspondence should be addressed. Telephone: (405) 325-2924. Fax: (405) 325-6111. E-mail: MAshby@ou.edu.

[1] Abbreviations: CCSD, coupled-cluster singles and doubles; EPO, eosinophil peroxidase; ESI-MS, electrospray ionization mass spectrometry; LPO, lactoperoxidase; MP2, Møller−Plesset level two; NMR, nuclear magnetic resonance; SCF, self-consistent field; SVD, singular-value decomposition; TZ2P, triple-ζ double polarization; UV, ultraviolet.

10.1021/bi061015y CCC: $33.50
Published on Web 09/26/2006

between alternative formulations for hypothiocyanite, nuclear magnetic resonance (NMR) (*16*−*19*, *21*) and mass (*14*, *18*) spectra have been collected and analyzed. Chronologically, ^{15}N NMR spectra were collected first by Modi et al. (*17*, *21*), and a subsequent theoretical study was performed by Sundholm in an effort to analyze the observed ^{15}N NMR chemical shift (*13*). The latter theoretical study by Sundholm also yielded computed magnetic shielding constants for ^{13}C, but they were not compared with ^{13}C NMR chemical shifts that had been previously measured experimentally (*19*). There have also been several ^{13}C NMR studies of hypothiocyanite that have appeared in the interim (*16*, *18*), but these studies do not refer to the earlier computational study by Sundholm. Sundholm concluded that his computed ^{15}N shielding constants were most consistent with a formulation of $OSCN^-$ (or possibly $ONCS^-$), but that conclusion was based upon experimental ^{15}N NMR spectra that are disputed herein. In addition to the aforementioned studies of the spectroscopic properties of hypothiocyanite in solution, there have been two gas-phase studies by mass spectrometry (*14*, *18*). Arlandson et al. have employed negative ion electrospray ionization mass spectrometry (ESI-MS) to identify the major stable products of the eosinophil peroxidase (EPO)-catalyzed oxidation of SCN^- by H_2O_2 (*18*). In addition to several unidentified contaminate ions, an ion at *m*/*z* 74 was observed that could correspond to hypothiocyanite, but this observation did not distinguish between the different possible isomers. In a recent study by Dua et al. (*14*), collision-induced mass spectra (CID) were obtained for molecular precursors that were selected to produce $OSCN^-$, $ONCS^-$, and $OCNS^-$. When combined with the aforementioned theoretical calculations, the CID spectra provide evidence that $OSCN^-$ is a product of the oxidation of SCN^- by H_2O_2, but it was suggested that some of the other ions that were observed by Arlandson et al. were possibly due to $ONCS^-$ (or other isomers). In addition to conflicting conclusions that arise when comparing the aforementioned theoretical and spectroscopic studies, we note that many of the experimental results that have been previously reported appear to be inconsistent with the estimated lifetimes of hypothiocyanite under the conditions used in the experiments (vide infra). In an effort to reconcile these inconsistencies, we have reexamined the UV spectra, the ^{13}C NMR spectra, and the ^{15}N NMR spectra that result when hypothiocyanite is synthesized. Importantly, in contrast to previous investigations, we employ kinetic methods to evidence the correlations between the spectroscopic signatures we attribute to hypothiocyanite.

MATERIALS AND METHODS

Reagents. All chemicals were ACS certified grade or better. Water was doubly distilled in glass. Sodium hydroxide solutions, mostly free of CO_2 contamination, were quantified by titration with a standardized hydrochloric acid solution using phenolphthalein as an indicator. The buffer solutions were prepared from solid Na_2HPO_4 or K_3PO_4. K_3PO_4 and NaSCN were used as received from Sigma-Aldrich. Na_2HPO_4 was used as received from Mallinckrodt. Deuterium oxide (99.9%) was obtained from Cambridge Isotope Laboratories. Thiocyanate stock solutions were prepared from solid NaSCN that was dried in a 150 °C oven to a constant weight. $KS^{13}CN$ and $KSC^{15}N$ were used as received from Cambridge Isotope Laboratories and Isotec, respectively. Hypochlorite (OCl^-) solutions were prepared by adding aliquots of Cl_2 to NaOH until the desired concentration was achieved. The concentration of OCl^- was determined spectrophotometrically at 292 nm ($\epsilon_{292} = 350\ M^{-1}\ cm^{-1}$). Hypobromite ($OBr^-$) solutions were prepared by adding Br_2 to ice-cold solutions of NaOH (*22*). Hypobromite solutions were standardized spectrophotometrically at 329 nm ($\epsilon_{329} = 332\ M^{-1}\ cm^{-1}$) and were used within 2 h to minimize errors due to decomposition.

Generation of $OSCN^-$ by the Enzyme-Catalyzed Reaction of SCN^- and H_2O_2 (Method I). The appropriate amounts of SCN^- and LPO were incubated in a 0.1 M iP buffer at 20 °C. The reaction was initiated by the addition of H_2O_2. Typical conditions were as follows: (a) for NMR experiments, 40 mM SCN^-, 0.1 M iP, 10 mM H_2O_2, and 4 μM LPO (pH 7.20), and (b) for UV−vis experiments, 1 mM SCN^-, 0.1 M iP, 1 mM H_2O_2, and 0.1 μM LPO (pH 6.5).

Generation of $OSCN^-$ by Hydrolysis of $(SCN)_2$ (Method II). $(SCN)_2$ was generated by the heterogeneous reaction of $Pb(SCN)_2$ with Br_2 in CCl_4. $Pb(SCN)_2$ was synthesized by mixing ice-cold aqueous solutions of $Pb(NO_3)_2$ and NaSCN. The resulting precipitate was filtered, washed with ice-cold water, and dried. The concentration of Br_2 in water-saturated CCl_4 was determined spectrophotometrically ($\epsilon_{400} = 160\ M^{-1}\ cm^{-1}$). Excess $Pb(SCN)_2$ was added to the CCl_4 solution of Br_2, and the resulting slurry was vortexed until the solution became colorless. The Pb salts were removed by centrifuging and decanting. The concentration of $(SCN)_2$ in CCl_4 was confirmed spectrophotometrically ($\epsilon_{296} = 140\ M^{-1}\ cm^{-1}$). An aliquot of the CCl_4 solution of $(SCN)_2$ was added to 0.1 M aqueous NaOH with vigorous stirring (the volume of the aqueous phase was at least 10 times the volume of the CCl_4 phase). The two-phase solution was vortexed for 1 min, and then the emulsion was separated into two phases by centrifugation (the top layer is the water phase).

Generation of $OSCN^-$ by Reaction of SCN^- and OX^- (Method III). The reaction of OX^- and SCN^- at pH 13 results in the formation of $OSCN^-$ in the presence of a sufficiently large excess of SCN^-. Turbulent mixing of the solutions is necessary to avoid locally high concentrations of OX^- that can result in overoxidation of SCN^-. Turbulent mixing was achieved by using a stopped-flow instrument, by using a quench-flow instrument, or by using a hand mixer comprised of two Hamilton syringes and a T-mixer. To obtain a stoichiometric amount of $OSCN^-$ for the measurement of its extinction coefficient, a 400-fold excess of SCN^- over OCl^- was necessary. For the NMR experiments, a 10-fold excess of SCN^- was employed, which results in a >50% yield of $OSCN^-$ (as determined by UV−vis spectroscopy at $\lambda = 376$ nm). The overoxidation products were not observed by NMR, and they did not appear to affect the lifetime of the ^{13}C and ^{15}N NMR spectra of $OSCN^-$. Typical conditions were as follows: (a) for NMR experiments, 200 mM SCN^-, 0.1 M OH^-, and 10 mM OX^-, and (b) for UV−vis experiments, 1 M SCN^-, 0.1 M OH^-, and 2.5 mM OX^-.

Synthesis of Isotopically Labeled $(SCN)_2$. The synthesis of $(SCN)_2$ was carried out using the procedure that is described in method II. $Pb(SCN)_2$ was synthesized with isotopically enriched SCN^- (97% $S^{13}CN^-$ and 98% $SC^{15}N^-$).

pH Measurements. The OH^- concentrations for the unbuffered solutions were determined by acid−base titration against standardized HCl solutions using phenolphthalein as

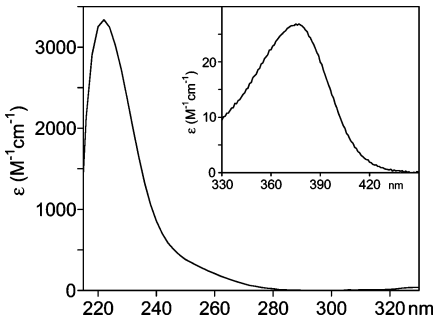

FIGURE 1: UV−vis spectrum that is assigned to $OSCN^-$ at pH 13. Thiocyanogen [0.5 mL of 11.5 mM $(SCN)_2$ in CCl_4] was extracted into a NaOH (10 mL of 0.1 M) solution to produce $OSCN^-$ (final concentration of 575 μM), and the composite UV spectrum (path length of 0.1 cm) was recorded 3 min later. The spectrum in this figure was obtained by subtraction of the spectrum of SCN^- (575 μM in 0.1 M NaOH). The inset shows the UV−vis spectrum observed when SCN^- (1 M) is reacted with OCl^- (1.28 mM) using a Bio-Logic stopped-flow apparatus (see Materials and Methods).

an indicator. The H^+ concentrations of the buffered solutions were determined with an Orion EA920 Ion Analyzer using an Ag/AgCl combination pH electrode.

UV−Vis Spectroscopy. Electronic spectra for $OSCN^-$ that was generated using methods I and II were measured using quartz cells with calibrated 1 mm, 2 mm, 1 cm, 5 cm, and 10 cm path lengths and a HP 8452A diode array spectrophotometer at 20 °C. Spectral deconvolution of the UV−vis spectra (Figure 1) by singular-value decomposition (SVD) was achieved using Specfit/32 (Spectrum Associates, Marlborough, MA). For method III, turbulent mixing of reagents was necessary to ensure the homogeneity of reaction mixtures in the time frame of the chemical reaction (to avoid overoxidation), and this was achieved by employing a Bio-Logic SFM-400/Q mixer. The UV−vis spectrum of the product of the reaction of OCl^- and SCN^- at pH 13 (Figure 1, inset) was recorded with a Bio-Logic MOS-450 monochromator with an ALX-250 Xe source and a PMS-250 photomultiplier detector. It required ca. 5 s to record the spectrum in the inset of Figure 1.

^{13}C NMR Measurements. The ^{13}C NMR measurements were taken with a Varian Inova 400 MHz NMR spectrometer at 100.57 MHz using a Varian four-nucleus switchable 5 mm probe while employing D_2O as a frequency lock. Chemical shifts were referenced to internal dioxane (66.6 ppm).

^{15}N NMR Measurements. The ^{15}N NMR measurements were taken with a Varian Inova 600 MHz NMR spectrometer at 60.79 MHz using a Varian broadband 5 mm probe while employing D_2O as a frequency lock. Chemical shifts were referenced to external NO_3^- (0.0 ppm).

RESULTS

Electron Spectrum of Hypothiocyanite. We have measured the composite UV spectrum that is produced upon generation of hypothiocyanite using methods I−III. These composite spectra have been analyzed by two distinctive approaches: (1) by employing blank solutions that comprised the constant components of the reaction mixtures (e.g., LPO, unreacted SCN^-, buffer, etc.) and (2) by factor analysis using singular-value decomposition (SVD). These two approaches produced essentially the same UV spectrum that is assigned to hypothiocyanite. That spectrum is very similar to those that have been previously measured (*15*, *20*), except for an additional feature at $\lambda_{max} = 376$ nm. The representative UV spectrum that is illustrated in Figure 1 was produced upon synthesis of hypothiocyanite by method II (inset of Figure 1 by method III). The composite spectrum was analyzed by the second approach (subtraction of a spectrum of SCN^-). The molar extinction coefficients that have been previously reported and those that have been measured in this study are summarized in Table 1.

^{13}C NMR Spectrum of Hypothiocyanite. We have measured the time-resolved ^{13}C NMR spectra that are produced upon generation of hypothiocyanite using methods I−III. For method I, we have measured the spectra at pH 7 (the pH at which catalysis occurs) as well as at pH 13. The latter was achieved by carrying out the catalysis at pH 7, which was complete within 1 min, followed by the turbulent mixing of sufficient NaOH to achieve a pH of 13. For method II, a solution of $(SCN)_2$ that was prepared in CCl_4 was added dropwise to a solution of 0.1 M NaOH while vortexing, followed by centrifugation to induce phase separation and transfer to the NMR tube. The preparative operation took approximately 3 min. For method III, the oxidation of SCN^- by HOX (X = Cl and Br) was achieved using turbulent mixing methods, and the spectra were measured both at pH 7 and at pH 13. The spectrum at pH 7 was recorded at 4 °C after a pH jump from pH 13 (the pH that was employed to synthesize hypothiocyanite). The observed ^{13}C NMR chemical shifts that have been previously reported and those that have been measured in this study are summarized in Table 2. Note that in the case of previous measurements, we have summarized in Table 2 the assignments for hypothiocyanite that were made by the original authors (as explained in the footnotes of Table 2), even though in some cases those assignments were apparently incorrect (vide infra).

^{15}N NMR Spectrum of Hypothiocyanite. We have measured the time-resolved ^{15}N NMR spectra that are produced upon generation of hypothiocyanite using methods I−III. For method I, we have measured the spectra at pH 7.2. After the generation of hypothiocyanite at 20 °C, the sample was transferred to a NMR probe that had been precooled to 4 °C, after which data collection was immediately begun. For method II, a solution of $(SCN)_2$ that was prepared in CCl_4 was added dropwise to a solution of 0.1 M NaOH while vortexing, followed by centrifugation to induce phase separation and transfer to the NMR tube. For method III, the oxidation of SCN^- by HOX (X = Cl and Br) was achieved

Table 1: Molar Extinction Coefficients for Hypothiocyanite

wavelength (nm)	extinction coefficient (M^{-1} s^{-1})	method of preparation	solvent	pH	ref
235	1.84×10^3	$LPO/H_2O_2/SCN^-$	27 mM P_i, 68 nM LPO	7.2	*15*
235	1.29×10^3	$(SCN)_2$	0.1 M P_i	8.0	*20*
235	1.48×10^3	$(SCN)_2$	NaOH	13	this work
376	26.5	method I	NaOH	13	this work

Table 2: Observed ^{13}C Chemical Shifts for Hypothiocyanite

chemical shift[a] [δ (ppm)]	method of preparation	solvent[f]	pH of NMR measurement	ref
128.5[b]	LPO/H_2O_2/SCN^-	0.1 M P_i	6.0	*19*
128.6[c]	LPO/H_2O_2/SCN^-	0.1 M P_i	7.0	*19*
128.6[d]	V-BPO/H_2O_2/SCN^-	0.1 M P_i	7.0	*16*
127.3[e]	EPO/H_2O_2/SCN^-	0.1 M P_i	6.0 and 7.4	*18*
127.7	LPO/H_2O_2/SCN^-	0.1 M P_i	7.2	this work
127.8	LPO/H_2O_2/SCN^-	0.1 M P_i → $NaOH_i$	13.0[f]	this work
127.8	$(SCN)_2$	NaOH	13.0	this work
127.8	OCl^-/SCN^-	NaOH	13.0	this work
127.7	OCl^-/SCN^-	NaOH → 0.1 M P_i	7.2[g]	this work
127.8	OBr^-/SCN^-	NaOH	13.0	this work

[a] For $OSCN^-$ as assigned in the original publications. [b] A resonance at 126.9 ppm is observed initially, which within 30 min decomposes to give the resonance at 128.5 ppm. The former is assigned to NCS−O−SCN^{2-} and the latter to $OSCN^-$. [c] A resonance at 127.5 ppm is observed initially, which eventually evolves into a resonance at 128.6 ppm. The former is assigned to NCS−O−SCN^{2-} and the latter to $OSCN^-$. [d] A resonance at 127.6 ppm is observed initially, which eventually evolves into a resonance at 128.6 ppm. The latter resonance was assigned to $OSCN^-$. [e] A resonance is also observed at 128.8 ppm, but this is attributed to OCN^-. When the resonance at 127.8 ppm disappears, the resonance at 128.8 ppm remains. [f] The catalysis was performed at pH 7, and then a pH jump to pH 13 was performed prior to the NMR measurement. [g] The oxidation was performed at pH 13, and then a pH jump to pH 7.2 was performed prior to the NMR measurement.

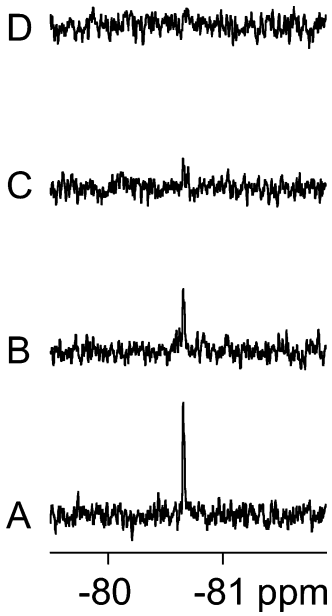

FIGURE 2: Time-resolved ^{15}N NMR spectra illustrating the resonance that is assigned to $OSCN^-$. The reaction was initiated by turbulent mixing of a solution of OCl^- (final concentration of 20 mM) with SCN^- (final concentration of 200 mM). Data collection was begun within 1 min of mixing. Each spectrum was obtained by averaging 64 transients, which required 35 min. Spectrum A was the first spectrum that was obtained (36 min after mixing). Spectra B−D were recorded at 35 min intervals. Thus, the half-life for disappearance of the resonance at −80.7 ppm is approximately 40 min, which is the same half-life that is observed for the disappearance of the UV spectrum and ^{13}C resonance that are assigned to $OSCN^-$ (see the text). NMR parameters: 20 °C, spectral window (sweep width) of 20000 Hz from −17917 to −2083 Hz that is equal to −295.4 to 34.3 ppm, $d_1 = 25$ s, pW = 35°, pH 13.

using turbulent mixing methods, and the spectra were measured both at pH 13 and at pH 7. The spectrum at pH 7 was recorded after a pH jump from pH 13 following the generation of hypothiocyanite under basic conditions at 4 °C. Figure 2 includes time-resolved ^{15}N NMR spectra that illustrate the disappearance of the resonance that we assign to hypothiocyanite with an approximate half-life that corresponds to the disappearance of the UV absorption band at $\lambda_{max} = 376$ nm. The observed ^{15}N NMR chemical shifts that have been previously reported and those that have been measured in this study are summarized in Table 3.

Table 3: Observed ^{15}N Chemical Shifts for Hypothiocyanite

chemical shift[a] [δ (ppm)]	method of preparation	solvent	pH	ref
−179	$(SCN)_2$	0.1 M P_i	6.1	*17*
−179	LPO/H_2O_2/SCN^-	0.1 M P_i	6.0	*17*
−173[b]	HRP/H_2O_2/SCN^-	0.1 M P_i	4.0	*21*
−80.3	LPO/H_2O_2/SCN^-	0.1 M P_i	7.2	this work
−80.6	$(SCN)_2$	NaOH	13.0	this work
−80.6	OCl^-/SCN^-	NaOH	13.0	this work
−80.1	OCl^-/SCN^-	NaOH → 0.1 M P_i	7.6	this work

[a] For $OSCN^-$ as assigned in the original publications (except as noted). [b] This resonance was assigned as $(SCN)_2$ in the original paper, but it is known that $(SCN)_2$ is unstable at pH > 4.

DISCUSSION

Electron Spectrum of Hypothiocyanite. An increase in absorbance at 235 nm during the LPO-catalyzed oxidation of SCN^- by H_2O_2 has often been noted (*23*), but deconvolution of the electronic spectrum of hypothiocyanite has proven to be problematic for many reasons, including the facts that hypothiocyanite is a transient species, it apparently exhibits an undistinguished absorption spectrum, and other components of the reaction mixtures that produce it absorb in the same region of the spectrum. Table 1 summarizes the molar extinction coefficients that have been previously reported. The first estimate of the molar extinction coefficient of hypothiocyanite at 235 nm (1.84×10^3 M^{-1} cm^{-1} at pH 7.2) was made by Hogg and Jago (*15*). A similar value was later obtained by Pruitt and Tenovuo (1.29×10^3 M^{-1} cm^{-1} at pH 8.0), albeit by a somewhat different method (*20*). Our estimation of the molar extinction coefficient of hypothiocyanite at 235 nm is comparable to these values. It is noteworthy that when hypothiocyanite is generated using methods I and III, its subsequent decomposition at pH 13 appears to be a clean first-order reaction ($t_{1/2} = 30$ min). In contrast, when hypothiocyanite is generated by method II, the decomposition reaction is not clean (no isosbestic points are observed in the UV spectrum) and at least three reactions were observed, both at low (0.5 mM) and at high (10 mM)

initial concentrations of hypothiocyanite. The nature of the decomposition products was also dependent upon the cycle time that was used to record the time-resolved spectra on the diode-arrayed spectrophotometer (i.e., how often the sample was exposed to the lamp), which suggests that photochemistry was also involved in the decomposition process when method II was employed to synthesize hypothiocyanite. Since similar erratic behavior is not observed when methods I and III are employed to synthesize hypothiocyanite, we suggest the (possibly photochemical) decomposition processes could be due to CCl_4 and/or lead salts that are likely extracted into the aqueous phase. It is problematic to record the spectrum of hypothiocyanite below 300 nm when hypothiocyanite is generated by methods I and III due to the necessary subtraction of a large background of LPO and/or SCN^-. Problems are also encountered when hypothiocyanite is generated by method II due to the apparent mixture of products that are obtained. Some of these impurities absorb significantly below 300 nm. In contrast to the difficulties that are encountered below 300 nm, the absorption at 376 nm (where a well-defined absorption maximum is observed) is more characteristic of hypothiocyanite. We speculate that the reason the absorption maximum at 376 nm has not been previously observed is the fact that the molar extinction coefficient at $\lambda_{max} = 376$ nm is only 26.5 M^{-1} cm^{-1}. Accordingly, it is difficult to observe this spectral feature at the concentrations of hypothiocyanite that have previously been produced using enzymatic methods (typically less than 1 mM) while employing a path length of 1 cm. However, the band at 376 nm (which is observed for all three methods we have employed to synthesize hypothiocyanite) is readily distinguished for higher concentrations and/or longer path lengths. We have also observed the band at 376 nm for the LPO/H_2O_2/SCN^- system using a spectrophotometric cell with a path length of 5 cm when 1 mM hypothiocyanite was generated. Parenthetically, we note that we have employed the LPO/H_2O_2/SCN^- system to synthesize higher concentrations of hypothiocyanite (up to 10 mM). Because of less interference by the absorption of SCN^- (a species that is also present in excess), we anticipate that the absorption at 376 nm will prove to be a practical advantage when monitoring hypothiocyanite spectrophotometrically.

^{13}C Spectrum of Hypothiocyanite. The experimental ^{13}C chemical shifts that have been previously reported (*16*, *18*, *19*) for hypothiocyanite are summarized in Table 2. Interpretation of the ^{13}C NMR spectra that are produced by the various methods that have been used to synthesize hypothiocyanite is complicated by the fact that the spectra are dynamic. This has led to considerable disagreement concerning the assignments of the resonances that are observed (*16*, *18*, *19*). Such assignments are also problematic, because reference spectra are not available for the short-lived transient species. Furthermore, reference spectra have not been obtained for some of the proposed stable products. Finally, we note that some of the resonances of interest are relatively close to one another. Slight differences in reaction conditions and, probably more significantly, the means of referencing the chemical shift scale may have lead to confusion. With regard to the last issue, our reference to the first new ^{13}C NMR resonance at 127.7 ppm for pH 7.2 (and at 127.8 ppm for pH 13) that is observed upon oxidation of SCN^- is assigned to 127.3−127.6 ppm by others (*16*, *18*, *19*). At pH ~7, the resonance at 127.7 ppm subsequently produces a new resonance at 128.8 ppm, which is reported to be 128.5−128.6 ppm by others (*16*, *18*, *19*). We have reasoned that sound assignment of the resonances could be achieved by correlating the temporal changes that occur in the ^{13}C NMR spectra with the other spectral signatures that have been attributed to hypothiocyanite, including, for example, the aforementioned UV spectrum. Toward this end, we have carried out parallel experiments in which the same solutions were monitored by UV spectroscopy and ^{13}C NMR spectroscopy. These measurements have permitted us to confirm the conclusion of Arlandson et al. (*18*) that the resonance at 127.7 ppm is due to hypothiocyanite and the subsequent development of a resonance at 128.8 ppm is due to cyanate (OCN^-). This is in contrast to previous assignments that attributed the resonance at 127.3 ppm to a precursor of hypothiocyanite (*16*, *19*).

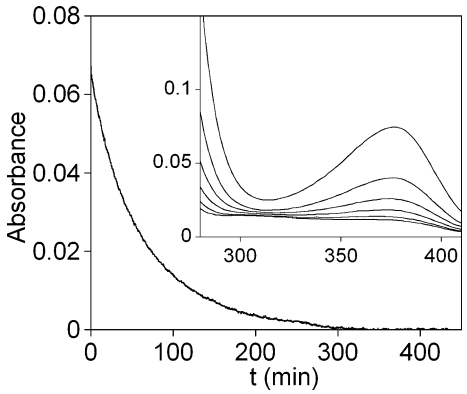

FIGURE 3: Change in absorbance that is observed at a representative wavelength (376 nm) upon addition of H_2O_2 (1 mM) to a solution of LPO (0.1 μM) and SCN^- (1 mM) in 0.1 M phosphate buffer (pH 6.5). The UV−vis spectra were recorded at time intervals of 20 s, but for clarity, the transient spectra are illustrated at intervals of 40 min in the inset. Fit of these data to a first-order rate law yields a k_{obs} of 2.72 × 10^{-4} s^{-1} and a half-life of 42.5 min. A similar rate constant is obtained for singular-value decomposition (SVD) analysis of the entire UV spectrum (inset). These were the conditions that were employed by Modi et al. to obtain the ^{15}N NMR spectra in Figure 4 of their work (*17*), which appears to show the resonance they assign to $OSCN^-$ after more than 60 half-lives.

^{15}N Spectrum of Hypothiocyanite. The experimental ^{15}N chemical shifts that have been previously reported (*17*, *21*) for hypothiocyanite are summarized in Table 3. It is clear that the resonances we attribute to hypothiocyanite are very different from those that have been reported by Modi et al. (*17*, *21*). Possible reasons for this discrepancy deserve comment. The same challenges exist for the measurement of ^{15}N NMR spectra that were described above for the ^{13}C NMR spectra. In addition, the ^{15}N nucleus is less sensitive, and it exhibits a longer relaxation time, which requires the incorporation of longer relaxation delays into the pulse sequence and subsequently longer signal averaging to obtain ^{15}N NMR spectra with a signal-to-noise ratio that is comparable to that achieved for the ^{13}C NMR spectra. In an effort to obtain spectra more quickly, it is common practice to use relatively narrow sweep widths, and this is particularly problematic because ^{15}N exhibits an unusually broad range of chemical shifts. Failure to use a sufficiently broad sweep width to capture all of the resonances can result in the fold-over of peaks. While in some cases the folded-over reso-

nances can be detected (because they tend to be out of phase with respect to the resonances that lie within the sweep width), such resonances will occasionally appear in-phase accidentally. While it is conceivable that this has occurred in the case of the spectra that are reported by Modi et al., we have not been able to conceive of a fold-over model that would explain their spectra. In addition to possible problems with sweep width, it is noteworthy that the relaxation times for the ^{15}N nuclei tend to be long, and this is particularly true for the small inorganic ions of this study, since efficient relaxation mechanisms are not expected. We have measured a ^{15}N NMR relaxation time of 40 s for SCN^-. Some of the ^{15}N NMR spectra that were reported by Modi et al. were collected in as little as 1 min (with <1 mM sample). It appears very likely that spin saturation would result for the conditions that are reported by Modi et al. It is unclear to us how any of the ^{15}N NMR spectra could have been measured by Modi et al. under the conditions that were reported. Furthermore, we have determined that hypothiocyanite is not stable in the time frame of many of the ^{15}N NMR spectra of Modi et al. that contain the resonance that these authors attribute to hypothiocyanite. For example, we have followed the kinetics of decomposition of hypothiocyanite using UV spectroscopy. Figure 3 illustrates the change in absorbance that is observed at a representative wavelength (376 nm) upon addition of H_2O_2 (1 mM) to a solution of LPO (0.1 μM) and SCN^- (1 mM) in 0.1 M phosphate buffer (pH 6.5). Fit of these data to a first-order rate law yields a k_{obs} of 2.72×10^{-4} s^{-1} and a half-life of 42.5 min. A similar rate constant is obtained for singular-value decomposition (SVD) analysis of the entire UV spectrum. The conditions that we employed to collect the data depicted in Figure 3 are the same conditions that were employed by Modi et al. to obtain the ^{15}N NMR spectra in Figure 4 of their publication (*17*), which appears to show the resonance they assign to hypothiocyanite (after more than 60 half-lives).

Chemical Structure of Hypothiocyanite. One motivation behind many of the spectroscopic and theoretical studies of hypothiocyanite has been the desire to characterize its structure. A comparison of experimental and computed NMR chemical shifts probably affords the best opportunity to differentiate between alternative structures. It is in principle possible to compute chemical shieldings (σ), which in turn can be converted to chemical shifts (δ) by the relationship $\delta_X = \sigma_{ref} - \sigma_X$. However, certain challenges that exist in computing σ deserve comment before we compare our experimental chemical shifts to those that have been predicted by theory. The isotropic shielding constants are comprised of diamagnetic and paramagnetic terms ($\sigma_{iso} = \sigma^d + \sigma^p$). The Ramsey equation describes the effects of magnetic fields on the two terms (*24*). The diamagnetic term (which derives its name from the fact that it induces shielding and upfield chemical shifts) is only dependent on the ground-state wave function and is therefore readily computed by quantum chemical methods (provided a sufficiently large basis set is employed in the calculation). In contrast, the paramagnetic term (which corresponds to deshielding and downfield chemical shifts) involves a field-induced mixing of the ground state with excited states and is thus significantly more difficult to access. Note that the paramagnetic term in this context does not have the same meaning as the term when it is applied to molecules that have unpaired electrons.

Table 4: Computed[a] and Experimental ^{13}C Chemical Shifts [δ (Parts per Million)] for Isomers of Hypothiocyanite

isomer	δ^{SCF}	δ^{MP2}	δ^{CCSD}
$OSCN^-$	135	137	133
$ONCS^-$	70	39	49[b]
$OCNS^-$	125	108	114[b]
experimental			128

[a] The computed chemical shifts were taken from ref *13*. [b] Chemical shifts at the CCSD we extrapolated for the $ONCS^-$ and $OCNS^-$ isomers using the relationship $\delta^{CCSD}_{isomer} = \sigma_{ref} - (\sigma^{MP2}_{isomer} - \sigma^{MP2}_{isomer} - \sigma^{SCF}_{isomer}/3)$, where $\sigma_{ref} = 188$ ppm for TMS.

Table 5: Computed[a] and Experimental ^{15}N Chemical Shifts [δ (Parts per Million)] for Isomers of Hypothiocyanite

isomer	δ^{SCF}	δ^{MP2}	δ^{CCSD}
$OSCN^-$	−46	−135	−90
$ONCS^-$	−200	−226	−217[b]
$OCNS^-$	−367	−384	−379[b]
experimental			−81

[a] The computed chemical shifts were taken from ref *13*. [b] Chemical shifts at the CCSD we extrapolated for the $ONCS^-$ and $OCNS^-$ isomers using the relationship $\delta^{CCSD}_{isomer} = \sigma_{ref} - (\sigma^{MP2}_{isomer} - \sigma^{MP2}_{isomer} - \sigma^{SCF}_{isomer}/3)$, where $\sigma_{ref} = -132$ ppm for NO_3^-.

Sundholm has computed the nuclear magnetic shieldings for the possible isomers of hypothiocyanite (as well as related species) at several different levels of theory (*13*). We will refer here only to those calculations that employed a triple-ζ double polarization (TZ2P) basis set, the largest basis set that was employed by Sundholm. With regard to the level of correlation, which is important in the context of computing the paramagnetic term, it is necessary to reference three levels of theory. In order of sophistication, those levels of correlation are Hartree−Fock self-consistent field (SCF), Møller−Plesset level two (MP2), and coupled-cluster singles and doubles (CCSD) theories. A comparison of these levels of theory clearly shows (e.g., in Table 5 of Sundholm's publication) that large basis sets (i.e., TZ2P) and CCSD are required to adequately describe chemical shieldings in this system (*13*). Unfortunately, Sundholm performed CCSD calculations on only the $OSCN^-$ (and not the $ONCS^-$ or $OCNS^-$) isomers of hypothiocyanite. However, as pointed out by Sundholm, the SCF chemical shieldings are in general too small, and the MP2 level overestimates the correlation correction by approximately one-third. Thus, in Table 4, we list the computed ^{13}C chemical shift of $OSCN^-$ (at the CCSD level) and the extrapolated computed ^{13}C chemical shifts of $ONCS^-$ and $OCNS^-$ (using the equation in the footnote). The corresponding computed and experimental ^{15}N chemical shifts are listed in Table 5.

Sundholm suggested that the ^{13}C chemical shieldings were sufficiently different that they might be used to differentiate the isomers of hypothiocyanite, although he made no comparison at the time. The value we (and others) have measured for hypothiocyanite (128 ppm) appears to be most consistent with the computed chemical shift for $OSCN^-$ (133 ppm), although the computed value for $OCNS^-$ (114 ppm) is also close. In contrast, the computed value for $ONCS^-$ appears to be well outside the error that might be expected for this calculation. Working with the value for the ^{15}N chemical shift that was reported (*17*, *21*) by Modi et al. (−179 ppm), Sundholm ruled out $OCNS^-$, but the computed

values for $OSCN^-$ (−90 ppm) and $ONCS^-$ (−217 ppm) differed from the experimental value of Modi et al. by 89 ppm (downfield) and −38 ppm (upfield), respectively (*13*). Sundholm concluded that medium and vibration corrections must account for the discrepancy, and ^{15}N NMR could not be used to differentiate the two isomers (*13*). However, the value of the ^{15}N NMR chemical shift that we report (−81 ppm) is very close to the computed value for $OSCN^-$ (−90 ppm) and very different from the values that are estimated for $ONCS^-$ (−217 ppm) and $OCNS^-$ (−379 ppm). Accordingly, we conclude that the observed ^{13}C and ^{15}N NMR chemical shifts are both consistent with the $OSCN^-$ formulation.

CONCLUSION

There have been many previous efforts to characterize the structure of the transient oxidation products of SCN^- that are produced by the $LPO/H_2O_2/SCN^-$ system. However, these studies have produced many inconstancies, particularly with respect to the spectroscopic signatures that are attributed to hypothiocyanite, the putative antimicrobial that is produced by the $LPO/H_2O_2/SCN^-$ (and other defensive peroxidase) systems. In an effort to resolve these inconsistencies, we have obtained UV absorption spectra and NMR spectra. Resolution of the questions that have surrounded the spectral signatures of hypothiocyanite has been made possible by correlating spectral changes that are observed during the formation and decomposition of hypothiocyanite. We have identified a new spectral feature in the optical spectrum of hypothiocyanite that may prove to be useful in future studies. With regard to the NMR spectra, our observations are essentially consistent with previous reports of the ^{13}C NMR spectrum of hypothiocyanite, but we cannot explain the ^{15}N NMR spectra that have been previously reported for hypothiocyanite (*17*, *21*). The temporal changes we observe for the ^{13}C and ^{15}N NMR resonance we have assigned to hypothiocyanite correlate with the changes in the UV spectrum. Furthermore, our observed ^{13}C and ^{15}N NMR chemical shifts are consistent with the computed values for $OSCN^-$ (*13*). We now find that the UV spectra, ^{13}C NMR spectra, and ^{15}N NMR spectra that are obtained for hypothiocyanite that has been prepared by all known procedures are self-consistent.

ACKNOWLEDGMENT

We are grateful to Dr. Margaret Eastman for her assistance with the ^{15}N NMR measurements.

REFERENCES

1. Pruitt, K. M., and Tenovuo, J. O. (1985) in *The Lactoperoxidase System: Chemistry and Biological Significance*, Immunology Series, Vol. 27, Marcel Dekker, New York.
2. Furtmueller, P. G., Jantschko, W., Regelsberger, G., Jakopitsch, C., Arnhold, J., and Obinger, C. (2002) Reaction of lactoperoxidase compound I with halides and thiocyanate, *Biochemistry 41*, 11895−11900.
3. Barnett, J. J., McKee, M. L., and Stanbury, D. M. (2004) Acidic aqueous decomposition of thiocyanogen, *Inorg. Chem. 43*, 5021−5033.
4. Ashby, M. T., Carlson, A. C., and Scott, M. J. (2004) Redox buffering of hypochlorous acid by thiocyanate in physiologic fluids, *J. Am. Chem. Soc. 126*, 15976−15977.
5. Nagy, P., Beal, J. L., and Ashby, M. T. (2006) Thiocyanate Is an Efficient Endogenous Scavenger of the Phagocytic Killing Agent Hypobromous Acid, *Chem. Res. Toxicol. 19*, 587−593.
6. Hoogendoorn, H., Piessens, J. P., Scholtes, W., and Stoddard, L. A. (1977) Hypothiocyanite ion: The inhibitor formed by the system lactoperoxidase-thiocyanate-hydrogen peroxide. I. Identification of the inhibiting compound, *Caries Res. 11*, 77−84.
7. Loevaas, E. (1992) Free radical generation and coupled thiol oxidation by lactoperoxidase/thiocyanate/hydrogen peroxide, *Free Radical Biol. Med. 13*, 187−195.
8. Thomas, E. L., and Aune, T. M. (1978) Lactoperoxidase, peroxide, thiocyanate antimicrobial system: Correlation of sulfhydryl oxidation with antimicrobial action, *Infect. Immun. 20*, 456−463.
9. Ashby, M. T., and Aneetha, H. (2004) Reactive sulfur species: Aqueous chemistry of sulfenyl thiocyanates, *J. Am. Chem. Soc. 126*, 10216−10217.
10. Leung-Toung, R., Li, W., Tam, T. F., and Karimian, K. (2002) Thiol-dependent enzymes and their inhibitors: A review, *Curr. Med. Chem. 9*, 979−1002.
11. Ihalin, R., Loimaranta, V., and Tenovuo, J. (2006) Origin, structure, and biological activities of peroxidases in human saliva, *Arch. Biochem. Biophys. 445*, 261−268.
12. Pyykko, P., and Runeberg, N. (1991) Calculated Properties of $OCNS^-$ and Related Species, *J. Chem. Soc., Chem. Commun.*, 547−548.
13. Sundholm, D. (1995) *Ab Initio* Study of Nuclear Magnetic Shieldings and Ultraviolet Spectra For Hypothiocyanite and Its Isomers: The Molecular Structure of Hypothiocyanite, *J. Am. Chem. Soc. 117*, 11523−11528.
14. Dua, S., Maclean, M. J., Fitzgerald, M., McAnoy, A. M., and Bowie, J. H. (2006) Is the Hypothiocyanite Anion $(OSCN)^-$ the Major Product in the Peroxidase Catalyzed Oxidation of the Thiocyanate Anion $(SCN)^-$? A Joint Experimental and Theoretical Study, *J. Phys. Chem. A 110*, 4930−4936.
15. Hogg, D. M., and Jago, G. R. (1970) The antibacterial action of lactoperoxidase. The nature of the bacterial inhibitor, *Biochem. J. 117*, 779−790.
16. Walker, J. V., and Butler, A. (1996) Vanadium Bromoperoxidase-Catalyzed Oxidation of Thiocyanate By Hydrogen-Peroxide, *Inorg. Chim. Acta 243*, 201−206.
17. Modi, S., Deodhar, S. S., Behere, D. V., and Mitra, S. (1991) Lactoperoxidase-Catalyzed Oxidation of Thiocyanate By Hydrogen-Peroxide: N-15 Nuclear-Magnetic-Resonance and Optical Spectral Studies, *Biochemistry 30*, 118−124.
18. Arlandson, M., Decker, T., Roongta, V. A., Bonilla, L., Mayo, K. H., MacPherson, J. C., Hazen, S. L., and Slungaard, A. (2001) Eosinophil peroxidase oxidation of thiocyanate. Characterization of major reaction products and a potential sulfhydryl-targeted cytotoxicity system, *J. Biol. Chem. 276*, 215−224.
19. Pollock, J. R., and Goff, H. M. (1992) Lactoperoxidase-catalyzed oxidation of thiocyanate ion: A carbon-13 nuclear magnetic resonance study of the oxidation products, *Biochim. Biophys. Acta 1159*, 279−285.
20. Pruitt, K. M., and Tenovuo, J. (1982) Kinetics of hypothiocyanite production during peroxidase-catalyzed oxidation of thiocyanate, *Biochim. Biophys. Acta 704*, 204−214.
21. Modi, S., Behere, D. V., and Mitra, S. (1991) Horseradish peroxidase catalyzed oxidation of thiocyanate by hydrogen peroxide: Comparison with lactoperoxidase-catalyzed oxidation and role of distal histidine, *Biochim. Biophys. Acta 1080*, 45−50.
22. Engel, P., Oplatka, A., and Perlmutter-Hayman, B. (1954) Decomposition of hypobromite and bromite solutions, *J. Am. Chem. Soc. 76*, 2010−2015.
23. Reiter, B., Pickering, A., and Oram, J. D. (1964) An inhibitory system, lactoperoxidase-thiocyanate-peroxide, in raw milk, *Microb. Inhib. Food, Proc. Int. Symp., 4th, 1964*, 297−305.
24. Jameson, C. J. (1996) Understanding NMR chemical shifts, *Annu. Rev. Phys. Chem. 47*, 135−169.

BI061015Y